Fluid structure interaction analysis of an hydrofoil

Conference Paper · May 2013

CITATIONS
3

READS
255

7 authors, including:

Corentin Lothode
Université de Rouen
22 PUBLICATIONS **53** CITATIONS
SEE PROFILE

Mathieu Durand
Sirli Innovations
37 PUBLICATIONS **255** CITATIONS
SEE PROFILE

Michel Visonneau
French National Centre for Scientific Research
285 PUBLICATIONS **2,009** CITATIONS
SEE PROFILE

Yann Roux
K-Epsilon
31 PUBLICATIONS **115** CITATIONS
SEE PROFILE

V International Conference on Computational Methods in Marine Engineering
MARINE 2013
B. Brinkmann and P. Wriggers (Eds)

FLUID STRUCTURE INTERACTION ANALYSIS OF AN HYDROFOIL

C. LOTHODE*, M. DURAND*, Y. ROUX*, L. DOREZ+, M. VISONNEAU†, A. LEROYER†

*K-Epsilon
Espaces Antipolis, 300 route des Crêtes - CS 70116
06902 Sophia-Antipolis, France
e-mail: mathieu@k-epsilon.com, web page: http://www.k-epsilon.com/

† Laboratoire de recherche en Hydrodynamique, Énergétique et Environnement Atmosphérique
École Centrale de Nantes
1 rue de la Noë BP 92101, 44321 Nantes Cedex 3, France
e-mail: alban.leroyer@ec-nantes.fr - web page: http://www.ec-nantes.fr/

+ Groupama Sailing Team
56100 Lorient
e-mail: loic@groupamasailingteam.com - web page: http://www.cammas-groupama.com/

Key words: Fluid Structure Interaction, VIV, RANSE, Racing Yacht

Abstract. In this paper, a dynamic computation of the Groupama 3 foil is performed. Foils are thin profiles, placed under the hull of a ship, allowing it to provide a lifting force. This study is placed in the context of the 2013 America's Cup, which will see the appearance of a new kind of high performance multihull.

At high speeds, the foils are subject to intense hydrodynamic forces and to movement due to the sea. The deformations are then sizable and there is a risk of ventilation, cavitation or vibration that could lead to important modification of the hydrodynamic forces or to the destruction of the foil. It is therefore necessary to quantify correctly its deformation and its response to dynamical efforts.

The foil/water interaction is a strongly coupled problem, due to the thickness of the object. In this paper, the problem is solved using a segregated approach. The main problems resulting of such a method are the numerical stability and remeshing. These problems are detailed and some results presented.

As a first test case, the simulation of a vortex excited elastic plate proposed by Hubner is presented. This case is very demanding in terms of coupling stability and mesh deformation.

Then, the foil of Groupama 3 is modelled in a simplified form without hull and free surface, and then in a more realistic conditions with free surface and waves.

1 Numerical method

The strategy used to solve the fluid structure interaction problem is a partitioned coupling between a fluid solver and a structural solver. The two solvers are described in the following as well as the coupling algorithm.

1.1 Fluid : ISIS-CFD

The solver ISIS-CFD included in FINE/Marine^{TM}is developed by the DSPM team of LHEEA laboratory. It solves the Reynolds-Averaged Navier-Stokes Equations in a strongly conservative way. It is based on the finite volume method and can work on structured or unstructured meshes with arbitrary polyhedrons [WKR$^+$11].

The velocity field is obtained from the momentum conservation equations and the pressure field is extracted from the incompressibility constraint. The pressure-velocity coupling is achieved through a SIMPLE-like algorithm. All the variables are stored in a cell-centered manner. Volume and surface integrals are evaluated with second order discretization. The time integration is an implicit scheme of order two. At each time step, an internal loop is performed (called a non-linear iteration) associated with a Picard linearization in order to solve the non-linearities of the Navier-Stokes equations.

The equations are formulated according to the Arbitrary Lagrangian Eulerian paradigm and therefore can easily take into account mesh deformations. Several turbulence models are implemented in ISIS-CFD. In this study, we used the SST-$k-\omega$ model [MKL03].

1.2 Structure: ARA

The solver ARA was developed by the company K-Epsilon during the project VOILE-nav [ABHD12]. The code was initially aimed at simulating the dynamic behaviour of sailboat rigs : sails, mast and cables.

A non-linear finite element method with a large deformation formulation is implemented. At each time step, an equilibrium between external and internal forces is sought between all the elements and forces acting on them. The elements receive as an input the position, the speed and the acceleration of each of its nodes. It can contain internal variables in the case of elastic deformation, and the element computes the derivatives of forces according to those variables. These derivatives are assembled into a mass matrix $[M] = \frac{\partial F}{\partial \ddot{x}}$, damping matrix $[D] = \frac{\partial F}{\partial \dot{x}}$ and stiffness matrix $[K] = \frac{\partial F}{\partial tx}$. The elements can be composed of different kind of finite elements (cable, beam, shell, membrane). It is also possible to use elements with a penalization method such as contact or sliding elements. In the coupling algorithm, the fluid-structure interface itself is considered as an element.

The time scheme used is the Newmark-Bossak scheme (second order accurate). This scheme has been chosen for its compromise between the necessary filtering of the high frequencies while maintaining the accuracy of the low frequencies. The scheme is conservative hence avoids numerical energy creation in case of large non-linearities.

1.3 Elements used

While numerous element types have been implemented in the structural code, in the present study, only beam elements are used. These elements are Timoshenko elements, with the hypothesis of small deformations. We therefore have a constant stiffness matrix in the local frame. Each beam element is defined thanks to two points (for position) and two quaternions (for the tangent directions). More details on the non-linear algorithm used can be found in [Dur12].

1.4 Coupling

The fluid-structure coupling leads to four problems:

- the continuity of constraints at the interface ;
- the deformation of the interface ;
- the deformation of the fluid mesh ;
- the coupling algorithm.

1.4.1 Continuity of constraints

The perfect continuity of constraints cannot be assured because of the difference between the fluid discretisation and the structural discretisation. Thus, a consistent method is used (see [Dur12]). The method corresponds to an integration of the forces on the fluid faces :

$$\boldsymbol{F}_M = \int_\Gamma (p\,\boldsymbol{n} + \tau \cdot \boldsymbol{n})\, d\Gamma$$

and then a projection of those efforts on the degree of freedom of the closest beam element.

1.4.2 Interface deformation

The fluid structure interface is entirely defined by the fluid faces. Each fluid node is projected onto the nearest beam elements in order to get a parameterized position of the projected point as well as a vector linked to the local frame of the beam. When the beam is deformed, the 3D deformation of the neutral axis is computed with the variation of the local frame from one end to the other end of the beam. The local frame evolves smoothly according to a cubic spline law. Therefore, the new fluid node position is computed from the new position of the neutral axis and its local frame (see FIGURE 1).

(a) Fluid node projection (red) on the beam (blue segment)

(b) Fluid node position is computed according to the neutral axis (cubic spline) and the local frame

Figure 1: Fluid structure interface deformation.

1.4.3 Mesh deformation

Following the interface deformation, the whole mesh of the fluid domain needs to be deformed. This deformation occurs at each coupling iteration. The number of call to this procedure being non-negligible, the mesh deformation needs to be fast. To do this, a new method was developed that propagates the deformation state to the fluid mesh. The algorithm is described more thoroughly in [Dur12]. The rigid displacement (translation and rotation) of each face of the interface is computed. This displacement is propagated to its neighbours and so on iteratively until the boundaries of the mesh are reached.

1.4.4 Quasi-monolithic algorithm

The global solution algorithm is based on a quasi-monolithic approach. This approach is an implicit coupling adapted to a partitioned solver while conserving the property of convergence and stability of the monolithic approach. To obtain such a result, the structural computation is performed at each non-linear iteration of the fluid (inner loop). The fluid algorithm is not modified. The non-linear iterations include a fluid subiteration and a structural convergence. The non-linear iterations are performed until convergence, therefore fluid-structure convergence is reached at each time step. Furthermore, an "interface" element is added to the structural solver. This element is computed from the Jacobian matrix of the interface. In the case of an exact Jacobian matrix, the algorithm is the same as a monolithic algorithm. With the same idea as the quasi-Newton method where a simplified Hessian matrix is used, here a simplified Jacobian is computed.

The Jacobian matrix is not necessary, even for strongly coupled problems. Nonetheless, its use permits the elimination of under-relaxation, implying a significant reduction in the number of coupling iterations required.

With the present method, the ratio between the time of fluid structure interaction and fluid only computation is in between 1 and 2.

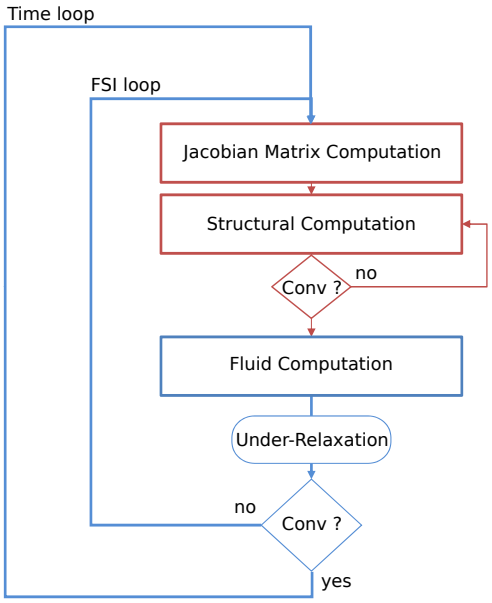

Figure 2: Dynamic coupling algorithm. In blue, the fluid solving scheme. In red, the added structural iteration with the Jacobian computation.

2 Test cases

2.1 Hubner test

To start, an academic test was studied [HWD04]. This case is itself a modification of [RW98] by changing certain boundary condition and characteristics of the structure. With the case of Hubner, the structure is more bendable and the deformations are larger. The case is therefore harder to study.

The parameters of Hubner were studied by Valdès et Vázquez [VMO09] and also by Guillaume De Nayer in 2008 [DN08]. The later modified the dimensions of the domain which he found to be too small. Those dimensions are used here (cf. FIGURE 3 and TABLE 1).

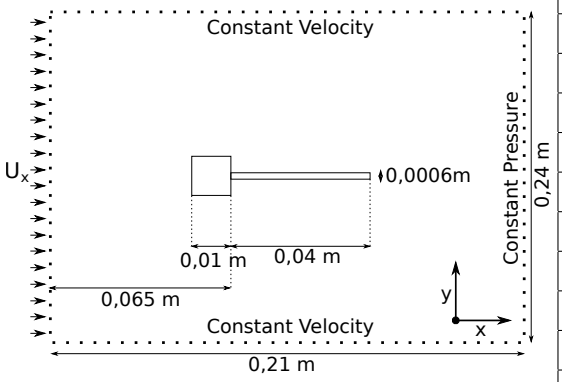

Figure 3: Diagram of the simulation

Fluid data			
Fluid density	ρ_f	$1,18$	$kg.m^{-3}$
Dynamic viscosity	μ_f	$1,82 \times 10^{-5}$	$Pa.s$
Inlet velocity	U_x	$0,315$	$m.s^{-1}$
Structural data			
Square size	a	$0,01$	m
Length of the tip	L	$0,04$	m
Tip thickness	d	$0,0006$	m
Young modulus	E	$0,2$	MPa
Tip density	ρ_s	2000	$kg.m^{-3}$
Poisson coefficient	ν	$0,35$	

Table 1: Properties of the fluid and the structure

According to the data, the Reynolds number is 200. The assumption of a laminar flow was used. The physical time of the computation is approximately 25 s and the time step is $\Delta t = 0.001s$. The fluid mesh was generated by HEXPRESS$^{\text{TM}}$, the mesher of the software FINE/Marine$^{\text{TM}}$. It has 111452 cells and 132782 vertices. The structural beam is made out of 100 beam elements.

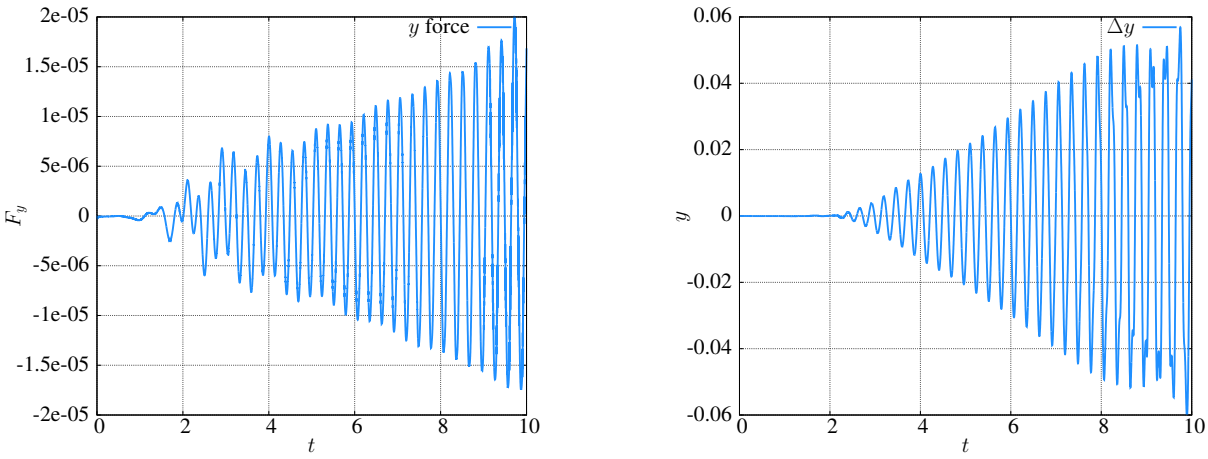

(a) y force (N) (b) y deflection (m)

Figure 4: Evolution of forces and deformation

The results obtained by Hubner show an amplitude of $6cm$ and correspond to the results obtained by the method presented here. Furthermore, the frequency $(3.15 \pm 0.05Hz)$ is also in the ranged obtained by Hubner and De Nayer ($3.22Hz$ for De Nayer, $3.10Hz$ for Hubner).

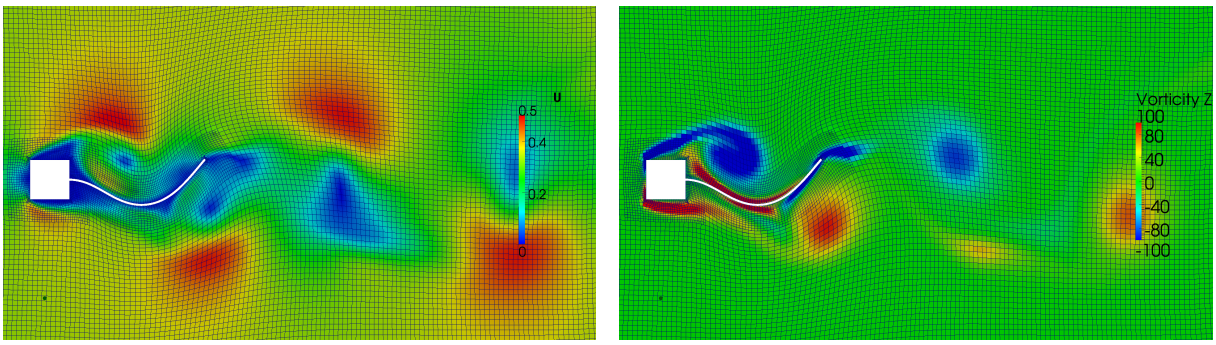

(a) $\| \boldsymbol{u} \|$ (b) ω_z

Figure 5: Visualization of the mesh deformation and creation of vortices in established flow

The FIGURE 5 shows the results of the mesh deformation. The cell quality and orientation is preserved even with relatively large deformation.

The tip oscillates in phazse with the creation of vortices by the square block. We can see those vortices advected in the flow FIGURE 5b.

2.2 Hydrofoil

A daggerbpard is providing side force to counter the force produced by the sail. Recently on multihulls, it iss also use to provide lift force, either as a lift assist foil[1] or a fully flighting foil[2]. Most of the time, the influence of the daggerboards can be modified by modifiying their orientation and position.

The study is done on the foil of Groupama 3, trimaran of 105 feet (32 m) and 18 tons. The boat broke the Jules Vernes record (fastest circumnavigation around the world) in 2010. This boat represents a break through in the concept of oceanic racing yachts by being lighter and by including hydrofoils.

[1]to reduce the drag by reducing the immersed volume of the hull, which is the case of most sailing multihulls

[2]hull out of the water, like the Hydroptère

Figure 6: Groupama 3

The foil used by Groupama 3 is a C foil, which is the shape you can see by looking at it by the front side. It also has a winglet to reduce the induced drag.

2.2.1 Foil alone

In this case, a simplified version of the foil is used. The foil is simply an extrusion of a NACA 4512 profile, with a curvature radius of $3m$, without the winglet. Furthermore, we do not take into account the free surface. The structural properties are listed below:

Length	4 m	Bending inertia (I_x)	7×10^6 mm^4
Width	0.7 m	Bending inertia (I_y)	1×10^9 mm^4
Mass	75 kg	Shear modulus (G)	3×10^4 MPa
Young modulus	2×10^5 MPa	Torsion inertia (I_0)	3×10^6 mm^4
Mean section area	8×10^3 mm^2		

Table 2: Simplified structural data

The structural mesh is given by 14 beam elements, with the node at the highest elevation blockfixed in position and rotation.

The first step is a quasi-static computation to predict the equilibrium position of the foil. Fluid iterations are performed alone until convergence, then a structural convergence is performed. The mesh is updated and a new fluid convergence with the new deformed mesh is performed. The quasi-static loop is done until convergence of the geometry. This convergence is assured only if the problem is stable.

The results obtained are in the TABLE 3. Those results were obtained with an inlet velocity of $15m \cdot s^{-1}$.

	Position z	z force
Undeformed foil	-1.351 m	7.434×10^4 N
Deformed foil	-0.756 m	9.316×10^4 N
Difference	0.595 m	1.882×10^4 N

Table 3: Differences between a computation with or without fluid structure interaction

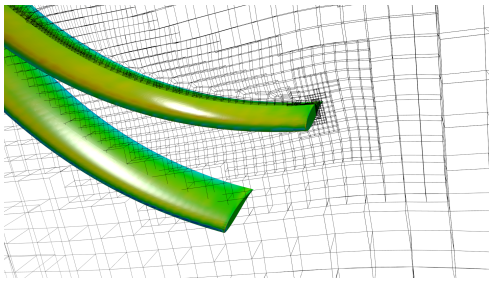

Figure 7: Undeformed and deformed foil and visualization of the deformed mesh

The gain in lift is big (+25%) whereas the drag is only augmented by a small factor (+3%) (see TABLE 3). By adjusting correctly the neutral axis and the center of effort, this behaviour can be optimized. At this speed, for a deformed foil, the lift represent 50% of the weight of the boat.

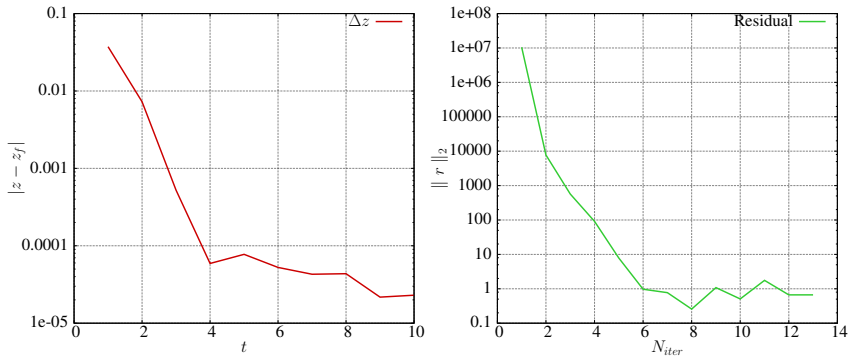

(a) Convergence to the solution

(b) Initial residual forces (before the structural computation is performed)

Figure 8: Convergence

The FIGURE 8 shows the quasi-static convergence. We notice that the deflection obtained is converged. The initial residual of the coupling (before computation of the structure) is decreasing by an order of magnitude at each coupling iteration. With only 6 quasi-static iterations, the solution is converged.

2.2.2 Foil with hull and waves

In this section, the real geometry of the foil (including the winglet) is used and the hull is added. Unsteady fluid structure interaction computations were performed with the foil fixed at the interface of the hull. A free surface is imposed at $z = 0$ as an initial condition. The hull is fixed and all of the nodes of the beam inside the hull are fixed in both translation and rotation.

At $t = 0$, the speed of the boat is 0. The imposed motion is done according to a $\frac{1}{4}$ sinusoidal law until $15m \cdot s^{-1}$. The waves are starting at $t = 0s$, $45m$ in front of the foil and reach the foil at $t = 6s$. The waves are Stokes first order potential waves 1 with $\pm 0.5m$ amplitude in z and a period of $3s$.

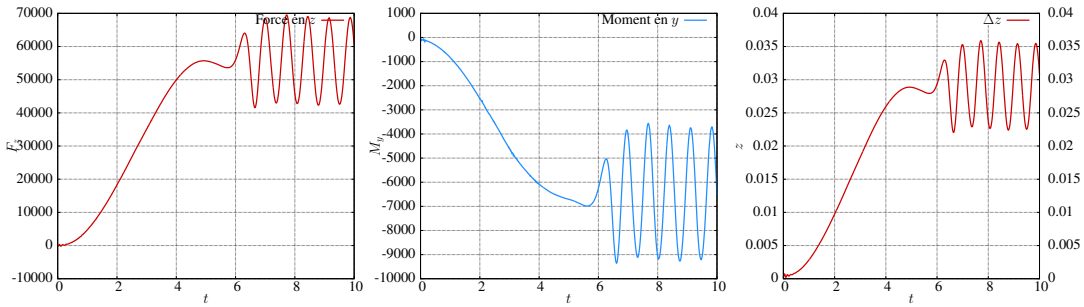

(a) z forces (b) y momentum (c) z deflection

Figure 9: Forces and momentum acting on the foil with respect to time

FIGURES 9a and 9b show the variation of the lift forces and torsion moment in the foil local frame. The variation of lift is $56 \pm 12 \times 10^3 N$.

The foil is very stiff and therefore does not bend very much. Nonetheless, the amplitude observed in waves is not negligible because it induce a vertical velocity that changes the incident flow, and thus the lift and drag.

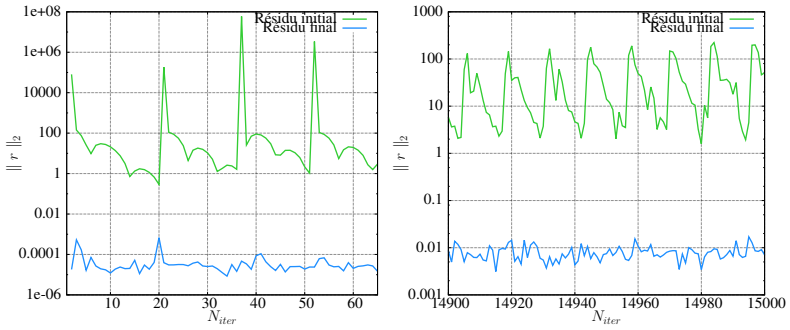

(a) Start of the simulation (b) End of the simulation

Figure 10: Initial residual on the structure

The FIGURE 10 permits us to conclude on the convergence of the coupling. It can be seen that the initial residual decreases quickly during the nonlinear iterations until convergence. Furthermore, using the Jacobian matrix of the interface allows a convergence in 20 subiterations where a classic implicit coupling with under-relaxation would require about a hundred subiterations. A computation without fluid structure interaction needs about 10 iterations to reach convergence.

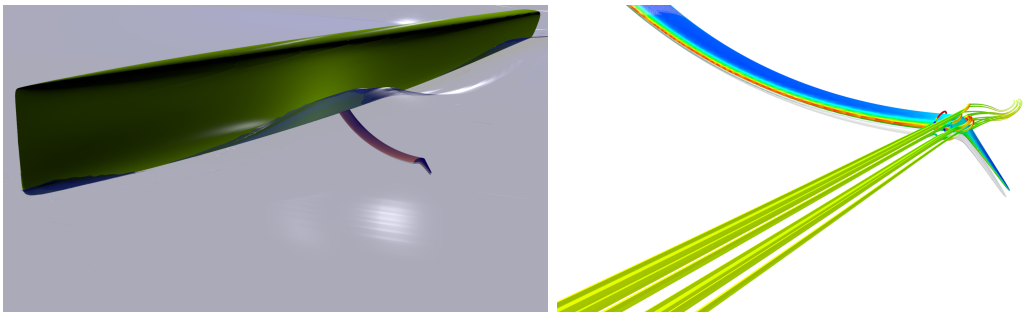

Figure 11: Computation results

Conclusion

The results of a partioned coupling between a viscous, incompressible fluid solver and a structural finite element analysis software are presented for strongly coupled problems. The Hubner case permitted the validation of the fluid-beam interaction. The quasi-static and dynamic results for the foil of a high performance multihull were then presented.

Furthermore, the design scope of this yacht was to do oceanic races and therefore it was designed to be both very reliable and safe. Thus, the foils used are smaller compared to what can be used for smaller, 60 foot (18 m) ORMA multihulls of the same generation. To use bigger foils on maxi trimaran, it will be necessary to predict the dynamic stability of the boat and also to dimension their structure.

Vibratory phenomena such as flutter, which can lead to structrual failure of the foil has not been investigated in the present study, but would of interest to determine the suceptiability to detrimental vibratory modes for the foil.

The boundary conditions for the structure play an important role in the determination of the structural deflections, hence it would be of interest to investigate a freely moving foil inside the hull with pinned connections at the lower and upper hull surfaces which corresponds more closely to what is happenning in reality.

Acknowledgment

We would like to thank PACAGrid and INRIA for providing the computational power required to undertake this study.

REFERENCES

[ABHD12] B. Augier, P. Bot, F. Hauville, and M. Durand, *Experimental validation of unsteady models for fluid structure interaction: Application to yacht sails and rigs*, Journal of Wind Engineering and Industrial Aerodynamics **101** (2012), 53–66.

[DN08] G. De Nayer, *Interaction fluide-structure pour les corps élancés.*, Ph.D. thesis, École Centrale de Nantes, 2008.

[Dur12] M Durand, *Interaction fluide-structure souple et legere, applications aux voiliers*, Ph.D. thesis, Ecole Centrale Nantes, 2012.

[HWD04] B. Hübner, E. Walhorn, and D. Dinkler, *A monolithic approach to fluid–structure interaction using space–time finite elements*, Computer methods in applied mechanics and engineering **193** (2004), no. 23, 2087–2104.

[MKL03] FR Menter, M. Kuntz, and R. Langtry, *Ten years of industrial experience with the sst turbulence model*, Turbulence, heat and mass transfer **4** (2003), 625–632.

[RW98] E. Ramm and WA Wall, *Fluid-structure interaction based upon a stabilized (ale) finite element method.*

[VMO09] J.G. Valdés, J. Miquel, and E. Oñate, *Nonlinear finite element analysis of orthotropic and prestressed membrane structures*, Finite Elements in Analysis and Design **45** (2009), no. 6–7, 395 – 405.

[WKR+11] J. Wackers, B. Koren, HC Raven, A. van der Ploeg, AR Starke, GB Deng, P. Queutey, M. Visonneau, T. Hino, and K. Ohashi, *Free-surface viscous flow solution methods for ship hydrodynamics*, Archives of Computational Methods in Engineering **18** (2011), no. 1, 1–41.